TOPIC HIGHLIGHT

WJG 20th Anniversary Special Issues (1): Hepatocellular carcinoma

DCE-MRI in hepatocellular carcinoma-clinical and therapeutic image biomarker

Bang-Bin Chen, Tiffany Ting-Fang Shih

Bang-Bin Chen, Tiffany Ting-Fang Shih, Department of Medical Imaging, National Taiwan University Hospital, Taipei 100, Taiwan
Bang-Bin Chen, Tiffany Ting-Fang Shih, Department of Radiology, National Taiwan University, Medical College, Taipei 100, Taiwan
Author contributions: Chen BB and Shih TTF reviewed related articles and wrote the manuscript.
Correspondence to: Tiffany Ting-Fang Shih, MD, Department of Medical Imaging, National Taiwan University Hospital, No.7 Chung-Shan S. Rd., Taipei 100, Taiwan. ttfshih@ntu.edu.tw
Telephone: 886-2-23123456 Fax: 886-2-23224552
Received: September 30, 2013 Revised: December 26, 2013
Accepted: January 20, 2014
Published online: March 28, 2014

Abstract

Dynamic contrast-enhanced magnetic resonance imaging (DCE-MRI) enables tumor vascular physiology to be assessed. Within the tumor tissue, contrast agents (gadolinium chelates) extravasate from intravascular into the extravascular extracellular space (EES), which results in a signal increase on T1-weighted MRI. The rate of contrast agents extravasation to EES in the tumor tissue is determined by vessel leakiness and blood flow. Thus, the signal measured on DCE-MRI represents a combination of permeability and perfusion. The semi-quantitative analysis is based on the calculation of heuristic parameters that can be extracted from signal intensity-time curves. These enhancing curves can also be deconvoluted by mathematical modeling to extract quantitative parameters that may reflect tumor perfusion, vascular volume, vessel permeability and angiogenesis. Because hepatocellular carcinoma (HCC) is a hypervascular tumor, many emerging therapies focused on the inhibition of angiogenesis. DCE-MRI combined with a pharmacokinetic model allows us to produce highly reproducible and reliable parametric maps of quantitative parameters in HCC. Successful therapies change quantitative parameters of DCE-MRI, which may be used as early indicators of tumor response to anti-angiogenesis agents that modulate tumor vasculature. In the setting of clinical trials, DCE-MRI may provide relevant clinical information on the pharmacodynamic and biologic effects of novel drugs, monitor treatment response and predict survival outcome in HCC patients.

Core tip: Dynamic contrast-enhanced magnetic resonance imaging (DCE-MRI) enables tumor vascular physiology to be assessed. Within the tumor tissue, contrast agents extravasate from intravascular into the extravascular extracellular space, which results in a signal increase on T1-weighted MRI. These signal intensity-time curves can be deconvoluted by mathematical modeling to extract parameters that may reflect tumor angiogenesis. DCE-MRI allows us to produce highly reproducible parametric maps of quantitative parameters in hepatocellular carcinoma (HCC). In the setting of clinical trials, DCE-MRI may provide relevant clinical information of novel drugs, monitor treatment response and predict survival outcome in HCC patients.

Chen BB, Shih TTF. DCE-MRI in hepatocellular carcinoma-clinical and therapeutic image biomarker. *World J Gastroenterol* 2014; 20(12): 3125-3134 Available from: URL: http://www.wjgnet.com/1007-9327/full/v20/i12/3125.htm DOI: http://dx.doi.org/10.3748/wjg.v20.i12.3125

INTRODUCTION

Hepatocellular carcinoma (HCC) is the sixth most common tumor and represents the third leading cause of cancer death worldwide[1]. It is the major cause of death in the cirrhotic patients, beside complications from portal hypertension[2]. The hypervascular nature and vascular in-out flow pattern of this tumor help differentiation of HCC from other tumors by non-invasive diagnostic criteria, without the necessity of tissue proof[3]. Like other malignant tumors, previous researches have reported the importance of angiogenesis with the development of HCC[4-8]. For example, Yamaguchi *et al*[9] found that vascular endothelial growth factor (VEGF) expression in HCC tissues may be related to the histological grade. Thus, various angiogenesis inhibitors have been developed to treat HCC. Among them, the multikinase inhibitor sorafenib was first approved and validated by two separate phase Ⅲ trials conducted in Western and Asian countries, respectively[10,11]. Up to December 2013, there are at least 20 active phase Ⅲ trials evaluating systemic treatments for advanced HCC (from clinicaltrials.gov-last visit 20th December 2013), with most of studies using sorafenib as combination therapy.

Dynamic contrast-enhanced magnetic resonance imaging (DCE-MRI) have been used widely as biomarkers in many early phase clinical trials to evaluate the effects of anti-angiogenic drugs that modulate tumor vasculature[12-16], and to help effective drug selection and optimal drug dose decision[17]. For phase Ⅲ clinical trials, DCE-MRI can serve as a surrogate biomarker to evaluate drug efficacy before the volumetric change of the tumor[18], and may be associated with progression-free survival and/or overall survival in these patients[19,20]. The enhancement patterns in HCC obtained by DCE-MRI are influenced by tumor angiogenesis and correlated with tumor microvessel density and VEGF expression[21]. Thus, suppression of tumor vascular permeability induced by anti-angiogenic agents can be reliably detected and quantified by DCE-MRI. Besides assessing anti-angiogenic agents, DCE-MRI can also be used in the evaluation of response of HCC after other treatments, including transarterial chemoembolization[22] and radiotherapy[23]. This review will attempt to summarize the current clinical application of DCE-MRI for HCC patients.

BASIS OF DCE-MRI

DCE-MRI images are obtained by injecting low-molecular-weight gadolinium chelated contrast agent into a vein with a constant rate[24]. The contrast agent is carried by blood flow into the tissue, causing increased signal intensity (SI) of the T1-weighted images due to the shortening of the longitudinal relaxation time of the tissue[25]. Within the tissue, the contrast agent passes from the arteries to the capillaries, and then extravasates to the extravascular extracellular space (EES). The rate of contrast agent extravasation to EES in the tumor tissue is determined by vessel leakiness and blood flow. Thus, the signal measured on DCE-MRI represents a combination of permeability and perfusion. DCE-MRI is sensitive to alterations in vascular permeability, extracellular space, and blood flow. To ideally record the signal change in the supplying blood vessel and within the tumor, a fast injection rate of the contrast agent captured with high temporal resolution is required[26,27].

This signal enhancement of liver perfusion can be quantified either with a semi-quantitative or quantitative analysis. The semi-quantitative analysis is based on the calculation of heuristic parameters that can be extracted from SI curves. In contrast, the quantitative analysis needs computational-based curve fitting algorithms using a bi-compartmental model with arterial input function. The parameters from both analysis methods have been shown to present correlation with tumoral angiogenesis[28].

SEMI-QUANTITATIVE ANALYSIS

Regarding the semi-quantitative analysis, different parameters that characterize the shape of the normalized SI-time curve can be extracted: (1) area under curve (AUC): expresses the amount of enhancement over a defined period of time (usually from starting increment of the SI-time curve to 60 or 90 s); (2) maximum of SI or Peak enhancement ratio ($SI_{maximun}$-$SI_{baseline}$/$SI_{baseline}$) of the enhancing curve; (3) wash-in Slope: determines the velocity of enhancement. It is calculated as the maximum change in enhancement per unit time, usually from 20% to 80% range of the increment curve; and (4) mean transit time (MTT): represents the mean time for blood to perfuse a region of tissue and is affected by the blood volume and blood flow in the region under analysis.

The semi-quantitative analysis is widely used because it is easy to calculate without the need of modeling. However, these heuristic parameters are highly affected by the gain factor of the acquisition systems, contrast media volume and injection rate, because the true concentration of contrast agent in the tissues is not estimated. Thus, differences in temporal resolution and injection rates can easily change the shape of SI curves, making comparison and quantification difficult[26,29]. Moreover, these descriptive parameters provide no physiologic insight into the behavior of the tumor vessels.

QUANTITATIVE ANALYSIS

On the other hand, the quantitative analysis is based on modeling the concentration change of the contrast agent using pharmacokinetic modeling techniques[30]. An initial conversion step of SI to concentration values is needed. Concentration *vs* time curves are then fitted using a bi-compartmental model (vessels and EES) with two vascular inputs (aorta and portal vein). The following parameters can be derived from a mathematical model[26,31]: (1) K^{trans} (forward volume transfer constant): determines the flux of the contrast agent from the intravascular space to the EES. It predominantly represents the vascular permeability in a permeability-limited (high flow) situation, but represents the blood flow into the tissue in a flow-limited

(high permeability) situation; (2) K_{ep} (reverse reflux rate constant): expresses the return process of the contrast agent from the EES to the intravascular space; and (3) V_e (volume fraction of EES): an indirect measure representing the cellular density of the tissue.

These parameters require additional calculations to generate parametric maps obtained after a pixel-by-pixel curve fitting process of the region under analysis. Thus, they are more computationally technical to obtain than the semi-quantitative ones. After generating parametric maps, the mean or median values within region of interests are usually calculated to represent tumor microvasculature, but histogram analysis[32] or heterogeneity in parametric maps[33-35] may also provide additional information. For optimum parameter quantification, a high temporal resolution is required to record initial rapid uprising of the SI curve immediately after the contrast agent administration[36]. The accuracy of these parameters is influenced by curve fitting algorithms[37,38] and magnitude of motion artifacts[39].

MODEL SELECTION

Kety[40] first described the flow-limited tracer uptake in tissue, and since then several pharmacokinetic models have been proposed by Tofts *et al*[41], Brix *et al*[42] and Larsson *et al*[43]. All these models used single source of arterial input function. Because HCC receives major blood supply from hepatic arteries, a single-input two compartment model is commonly used in most articles. However, for liver parenchymal disease or metastatic hepatic tumors which are supplied by both hepatic arteries and portal veins, a dual-input one compartment model by Materne *et al*[44] is often used to obtain parameters including arterial blood flow, portal blood flow, hepatic arterial fraction, distribution volume and MTT. For example, several articles used DCE-MRI with Materne model to stage liver fibrosis[45,46]. Liver perfusion assessed by DCE-MRI revealed increased hepatic arterial fraction and distribution volume with increasing liver fibrosis[45,47,48].

Recently, a hepatocyte-specific contrast agent was developed and showed different characteristics from traditional gadolinium-based contrast agents. A new model was developed for analysis of hepatic uptake by DCE-MRI using this hepatocyte-specific contrast agent[49]. Depending on the mathematical model applied and physiological assumptions made, variants of such quantitative parameters are obtained. Hence, when applying tracer kinetic modeling to clinical studies, it is important to state the choice of kinetic model employed at the outset. Currently, there is no consensus as to which kinetic model is best suited to evaluate the liver and HCC, and the development of an international consensus is necessary to allow a wider use of this technique.

Different field strengths employed in the dynamic acquisitions for developing DCE-MRI analysis have been shown to have a direct effect on the results of the pharmacokinetic parameters[50,51]. The choice of contrast agent molecular properties[52] and the temporal resolution of the acquisition have a clear influence on the parameters. To standardize calculations, the acquisition should have enough temporal resolution (less than 2-5 s each image set, during at least 5 min), and voxel-wise statistical analysis is suggested.

CLINICAL APPLICATION OF DCE-MRI

DCE-MRI is helpful to differentiate HCC from colorectal metastasis[53]. The values of arterial, portal and total blood flow, and distribution volume were significantly higher in the HCC than in the metastatic group, whereas MTT was significantly higher in the metastatic group.

Miyazaki *et al*[54] demonstrated that a lower pretreatment distribution volume and high arterial flow fraction was associated with a better response to treatment in patients with neuroendocrine liver metastases treated using yttrium-90 (Y-90)-labeled octreotide (^{90}Y-DOTATOC).

DCE-MRI is emerging as a promising method for monitoring tumor response to treatment in HCC patients, and could be used an early imaging biomarker to predict survival outcome of patients. The data are summarized in Table 1.

Wang *et al*[55] evaluated thalidomide efficacy in seven patients with advanced unresectable HCC that had failed to respond to prior local therapy. When comparing the MRI parameters for the tumors before and during treatment, they found a statistically significant difference for the peak enhancement, the maximal enhancement, and the enhancement slope percentage between two groups of patients (four had progressive disease, three had stable disease/partial response) with different clinical outcomes.

Liang *et al*[23] investigated the changes of the hepatic parenchyma and tumors by DCE-MRI in 19 patients with advanced HCC who received radiotherapy for 50 Gy in 25 fractions. An increased slope and peak of the tumor at week 2 was associated with an improved local response ($P < 0.05$) (Figures 1 and 2). In the parenchyma, an increased slope at week 2 was associated with recurrence outside the radiation fields or with progression over distant sites ($P < 0.05$). These findings emphasized the value of DCE-MRI in the second week after the start of radiotherapy in predicting local tumoral responses or systemic metastasis of HCC after radiotherapy.

Zhu *et al*[56] conducted a phase II study of sunitinib, an anti-VEFG receptor tyrosine kinase inhibitor, in 34 patients with advanced HCC. They found significant decreases in K^{trans} and K_{ep} after treatment ($P < 0.0001$). The extent of decrease in K^{trans} was substantially higher in patients who experienced partial response or stable disease compared with that in patients with progressive disease or who died during the first two cycles of therapy. They concluded that rapid changes in tumor vascular permeability are potential determinants of response and resistance to sunitinib in HCC.

Jarnagin *et al*[21] reports the results of 34 patients (26 intrahepatic cholangiocarcinoma and eight HCC) who received hepatic arterial infusion with floxuridine and dexamethasone. Patients with high pretreatment AUC had a lon-

Table 1 Summary of different hepatocellular carcinoma treatment, dynamic contrast-enhanced magnetic resonance imaging parameters and outcome

Ref.	Case number	Treatment	Parameter	Time interval	Outcome measure	*P* value
Wang *et al*[55], 2004	7	Thalidomide	↓ Peak, ↓ Slope	8 wk	P *vs* NP	< 0.05
Liang *et al*[23], 2007	19	Radiotherapy	↓ Peak, ↓ Slope	2 wk	R *vs* NR	< 0.05
Zhu *et al*[56], 2009	34	Sunitinib	↓ K^{trans}	2 wk	P *vs* NP	< 0.05
Jarnagin *et al*[21], 2009	34 (26 ICC and 8 HCC)	Floxuridine (FUDR) and dexamethasone	High baseline AUC, ↓ K$_{ep}$	2 mo	OS OS	0.002 0.013
Yopp *et al*[57], 2011	17 (14 and 3 HCC)	Floxuridine (FUDR) Bevacizumab	↓ AUC	2 wk	TTP	0.002
Hsu *et al*[58], 2011	31	Sorafenib, TG/uracil	High baseline K^{trans}	-	P *vs* NP	0.008
Hsu *et al*[58], 2011	31	Sorafenib, TG/uracil	↓ K^{trans}	2 wk	P *vs* NP OS PFS	0.003 0.015 0.030
Hsu *et al*[59], 2012	67	Vandetanib	↓ K^{trans}	1 wk	Pre *vs* Post	NS

HCC: Hepatocellular carcinoma; ICC: Intrahepatic cholangiocarcinoma; TG: Tegafur; P: Progression; NP: Non-progression; R: Responder. NR: Non-responder; PFS: Progression-free survival; OS: Overall survival; TTP: Time to progression; Pre: Pre-treatment; Post: Post-treatment; AUC: Area under curve; NS: Non-significant.
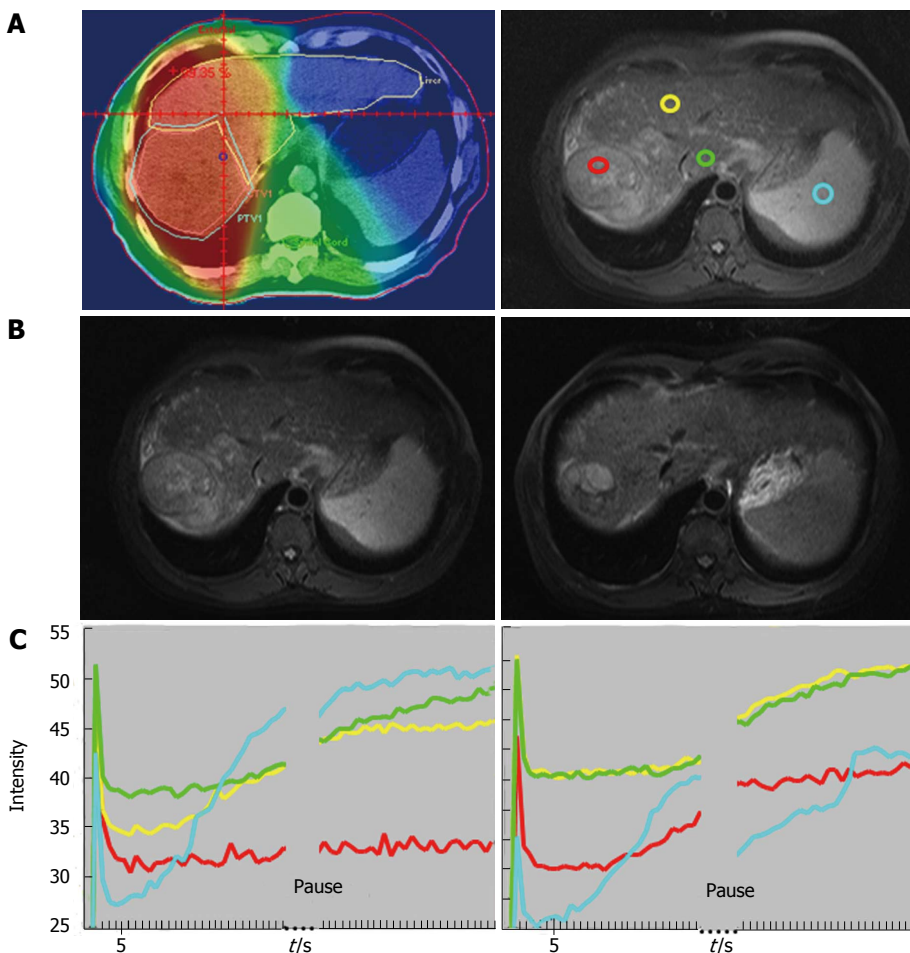
Figure 1 Forty-nine-year-old man with good local response. A: Isodose distribution and region of interests (ROIs): Left panel: Isodose distribution on center section of radiation treatment planning. Red: 45 Gy; orange: 40 Gy; yellow: 30 Gy; green: 15 Gy and blue: < 15 Gy. Right panel: ROIs on MRI before RT: red: tumor with strongest enhancement; yellow: non-tumor liver parenchyma receiving 30 Gy; green: non-tumor liver parenchyma receiving 15 Gy; blue: spleen; B: T1 weighted contrast-enhanced MRI before RT (left panel, the site corresponding to the right panel of (A) and after RT (right panel). Arrows indicate tumor margins; C: Time Intensity Curve of ROIs before RT (left panel) and at week 2 of RT (right panel). Red: tumor; yellow: 30 Gy; green: 15 Gy; blue: spleen. The curve of spleen is deviated after pause for respiration due to interference by lung perfusion. The initial spike due to refocusing artifact will not be counted into analysis. (From reference [23], reprint with permission).
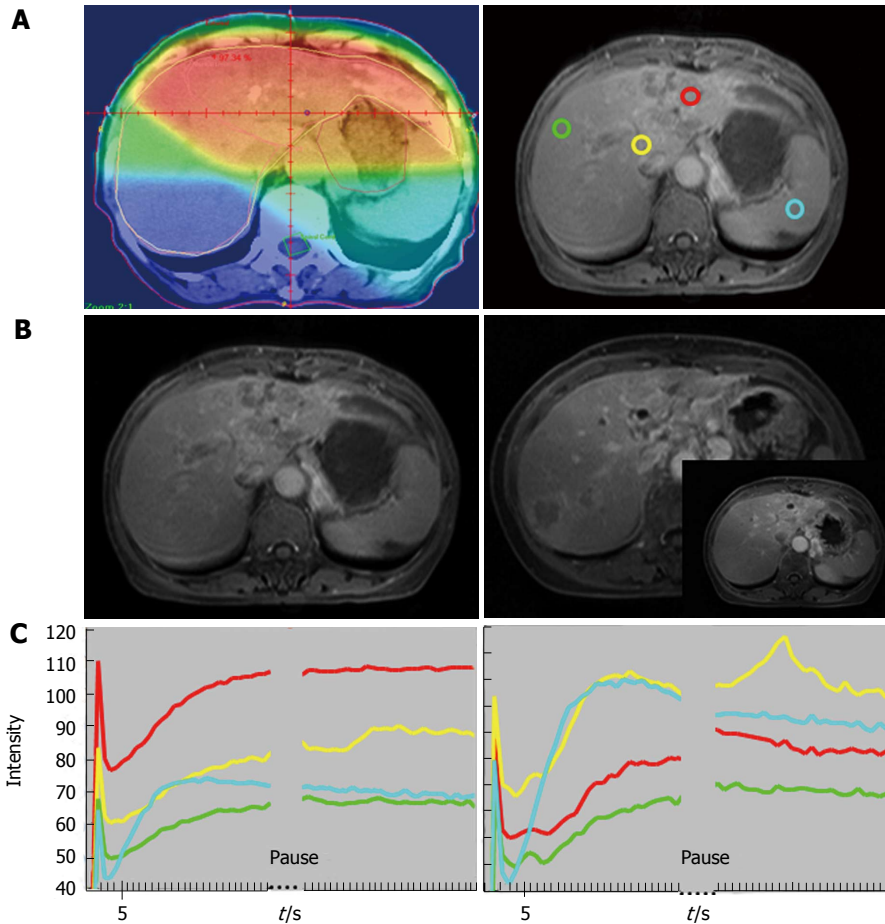
Figure 2 Sixty-four-year-old woman with good local response and intrahepatic recurrence outside of RT fields. A: Isodose distribution and region of interests (ROIs): Left panel: isodose distribution on center section of radiation treatment planning. Red: 45 Gy; orange: 40 Gy; yellow: 30 Gy; green: 15 Gy; blue: < 15 Gy. Right panel: ROIs on magnetic resonance imaging (MRI) before RT: red: tumor with strongest enhancement; yellow: non-tumor liver parenchyma receiving 30 Gy; green: non-tumor liver parenchyma receiving 15 Gy; blue: spleen; B: T1 weighted contrast-enhanced MRI before RT (left panel, same site as the right panel of (A) and after RT (right panel). The intersect picture of MRI over right panel demonstrates no tumor progression in the RT field on the center section of treatment planning. Arrows indicate tumor margins and arrowhead, recurrent tumor outside the field of RT; C: Time Intensity Curve of ROIs before RT (left panel) and at week 2 of RT (right panel). Red: tumor; yellow: 30 Gy; green: 15 Gy; blue: spleen. The initial spike due to refocusing artifact will not be counted into analysis. (From reference [23], reprint with permission).

ger median survival than those with low AUC ($P = 0.002$). Besides, decreased K^{trans} and K_{ep} on the first post-treatment MR scanning both predicted survival. Hence, pretreatment and early post-treatment changes in tumor perfusion characteristics may predict treatment outcome ahead.

Yopp *et al*[57] evaluated 17 patients (14 intrahepatic cholangiocarcinoma and 3 HCC) treated with floxuridine and bevacizumab. Significant decreases in AUC and K^{trans} were noted in tumors after bevacizumab. Time to progression correlated inversely with changes in AUC after bevacizumab. Reductions in tumor perfusion were greater in tumors expressing markers of anti-hypoxia and VEGF.

In one study of locally advanced HCCs receiving sorafenib and cytotoxic therapy, conducted by Hsu *et al*[58], a decrease of K^{trans} by 40% or greater after 14 days of treatment was correlated with longer progression free survival (PFS) and overall survival (OS). Besides, percentage of K^{trans} change (difference between pre- and post-treatment) is an independent predictor of tumor response, PFS, and OS (Figures 3 and 4). In another study, Hsu *et al*[59] reported a randomized clinical trial of 67 HCC patients

with vandetanib treatment, but no significant vascular change was found 1 wk after treatment. They explained that the steady-state concentration of vandetanib will be reached after at least 4 wk of treatment. Besides, the vascular features of heterogeneous nature of HCC due to tumor necrosis, arterio-venous shunting within the tumors, and the effects of prior local therapy, might preclude a reliable MRI measurement and comparison.

HCC EVALUATED BY PERFUSION CT

Similar to DCE-MRI, perfusion CT imaging of the liver is performed by acquisition of serial images after contrast bolus injection to obtain various perfusion indices, including regional tumor blood flow, blood volume, flow-extraction product, and permeability-surface area product. Previous reports have suggested that CT perfusion parameters can be used for quantifying tumor vascularity[60-64] and angiogenesis[65] in HCC, or as biomarkers to monitor response to chemoembolization[50], chemotherapy and a range of different targeted agents[66-68]. For ex-
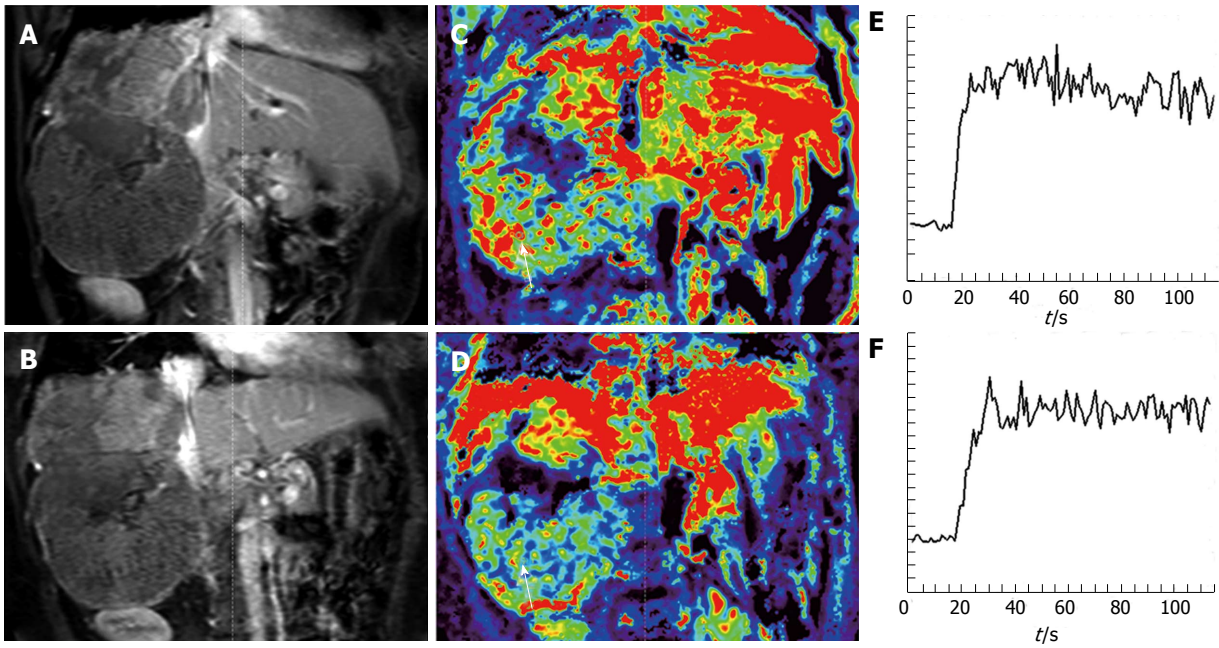
Figure 3 Representative dynamic contrast-enhanced magnetic resonance imaging findings in one advanced hepatocellular carcinoma patient. A: Post-contrast T1-weighted magnetic resonance imaging at baseline; B: After 14 d of study treatment; C: Corresponding color K^{trans} maps at baseline; D: After 14 d of study treatment. Hypervascular area was indicated by red color. The selected region of interest for K^{trans} measurement was indicated by white arrows. In this patient, the K^{trans} values at baseline and after study treatment were 798.6×10^{-3}/min and 206.6×10^{-3}/min, respectively; E: The initial area under the gadolinium concentration-time curves (IAUC) at baseline; F: After study treatment from the same patient. The IAUC values at baseline and after study treatment were 1526.2 mmol/kg $\times$ s and 1376.1 mmol/kg $\times$ s, respectively. (From reference [58], reprint with permission).
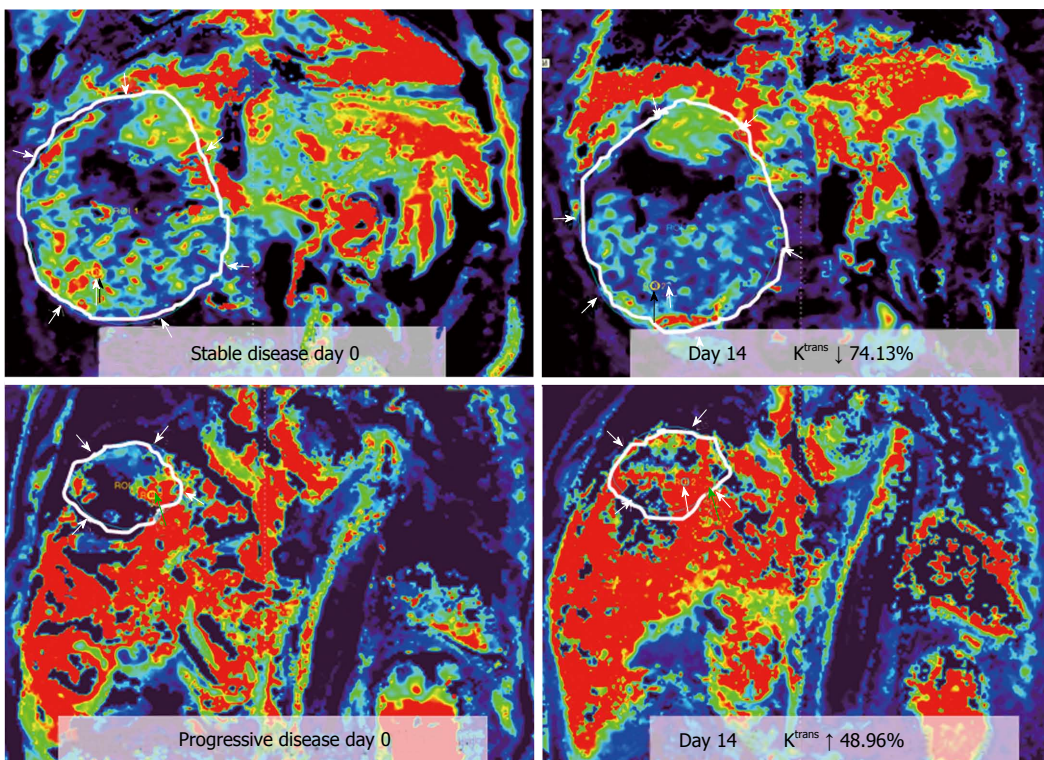
Figure 4 Representative dynamic contrast-enhanced magnetic resonance imaging K^{trans} color maps before treatment (day 0, left hand side) and day 14th after treatment (right hand side) in two advanced hepatocellular carcinoma patients. Corresponding hypervascular area was indicated by red color. region of interests analysis is more sensitive based on hypervascular part than entire tumor, with mean values. K^{trans} is a good diagnostic biomarker in differentiation between stable disease (SD, upper row) and progressive disease (PD, lower row) in two patients with hepatocellular carcinoma. Difference of K^{trans} (ΔK^{trans}) between SD and PD measured on hypervascular part and entire tumor are both significant. (From reference [58], reprint with permission).

ample, in one study of locally advanced HCCs receiving bevacizumab and cytotoxic therapy, high pretreatment K^{trans} by perfusion CT indicated those patients with a RECIST response[67]. Their findings were comparable with the results investigated by Hsu *et al*[58]: in patients with locally advanced HCCs receiving sorafenib and cytotoxic therapy, high pre-treatment K^{trans} measured by DCE-MRI indicated those patients who did not develop progressive disease[58]. The main drawback of perfusion CT is radiation exposure, but recent advances in multidetector CT technology many help achieve acceptable radiation dose in HCC patients.

FUTURE DIRECTION

Dynamic contrast-enhanced MR imaging is a reproducible technique. According to previous studies, the reproducibility of K^{trans} is good to moderate (coefficient of repeatability ranges from about 15%-40%)[69,70]. This suggests that in a well-conducted study, a change of K^{trans} value of more than 40% is likely to indicate a significant drug effect[71]. The reproducibility of DCE-MR imaging parameters is influenced by lesion location, with the parameters being significantly more reproducible in the liver than in the lung[72]. However, current DCE-MRI technique lacks standardization across multiple MR platforms and institutions, making it difficult to implement the technique in a multicenter setting[17,73]. Besides, there is a need to establish clear thresholds for a significant response when using quantitative DCE-MR imaging parameters for assessment of therapy response.

CONCLUSION

DCE-MRI is an imaging technique that appears to provide quantitative and biologically relevant informations related to tumor vasculature and angiogenesis, which can inform novel drug efficacy, monitor treatment response and act as an imaging biomarker to predict treatment outcome and survival in HCC patients.

REFERENCES

1   **Jemal A**, Bray F, Center MM, Ferlay J, Ward E, Forman D. Global cancer statistics. *CA Cancer J Clin* 2011; **61**: 69-90 [PMID: 21296855 DOI: 10.3322/caac.20107]

2   **Talwalkar JA**, Kamath PS. Influence of recent advances in medical management on clinical outcomes of cirrhosis. *Mayo Clin Proc* 2005; **80**: 1501-1508 [PMID: 16295030 DOI: 10.4065/80.11.1501]

3   **Bruix J**, Sherman M. Management of hepatocellular carcinoma. *Hepatology* 2005; **42**: 1208-1236 [PMID: 16250051 DOI: 10.1002/hep.20933]

4   **Kong SY**, Park JW, Lee JA, Park JE, Park KW, Hong EK, Kim CM. Association between vascular endothelial growth factor gene polymorphisms and survival in hepatocellular carcinoma patients. *Hepatology* 2007; **46**: 446-455 [PMID: 17659575 DOI: 10.1002/hep.21720]

5   **Poon RT**, Ho JW, Tong CS, Lau C, Ng IO, Fan ST. Prognostic significance of serum vascular endothelial growth factor and endostatin in patients with hepatocellular carcinoma. *Br J Surg* 2004; **91**: 1354-1360 [PMID: 15376182 DOI: 10.1002/bjs.4594]

6   **Chao Y**, Li CP, Chau GY, Chen CP, King KL, Lui WY, Yen SH, Chang FY, Chan WK, Lee SD. Prognostic significance of vascular endothelial growth factor, basic fibroblast growth factor, and angiogenin in patients with resectable hepatocellular carcinoma after surgery. *Ann Surg Oncol* 2003; **10**: 355-362 [PMID: 12734082]

7   **von Marschall Z**, Cramer T, Höcker M, Finkenzeller G, Wiedenmann B, Rosewicz S. Dual mechanism of vascular endothelial growth factor upregulation by hypoxia in human hepatocellular carcinoma. *Gut* 2001; **48**: 87-96 [PMID: 11115828]

8   **Park YN**, Kim YB, Yang KM, Park C. Increased expression of vascular endothelial growth factor and angiogenesis in the early stage of multistep hepatocarcinogenesis. *Arch Pathol Lab Med* 2000; **124**: 1061-1065 [PMID: 10888784 DOI: 10.1043/0003-9985(2000)124<1061]

9   **Yamaguchi R**, Yano H, Iemura A, Ogasawara S, Haramaki M, Kojiro M. Expression of vascular endothelial growth factor in human hepatocellular carcinoma. *Hepatology* 1998; **28**: 68-77 [PMID: 9657098 DOI: 10.1002/hep.510280111]

10 **Llovet JM**, Ricci S, Mazzaferro V, Hilgard P, Gane E, Blanc JF, de Oliveira AC, Santoro A, Raoul JL, Forner A, Schwartz M, Porta C, Zeuzem S, Bolondi L, Greten TF, Galle PR, Seitz JF, Borbath I, Häussinger D, Giannaris T, Shan M, Moscovici M, Voliotis D, Bruix J. Sorafenib in advanced hepatocellular carcinoma. *N Engl J Med* 2008; **359**: 378-390 [PMID: 18650514 DOI: 10.1056/NEJMoa0708857]

11 **Cheng AL**, Kang YK, Chen Z, Tsao CJ, Qin S, Kim JS, Luo R, Feng J, Ye S, Yang TS, Xu J, Sun Y, Liang H, Liu J, Wang J, Tak WY, Pan H, Burock K, Zou J, Voliotis D, Guan Z. Efficacy and safety of sorafenib in patients in the Asia-Pacific region with advanced hepatocellular carcinoma: a phase III randomised, double-blind, placebo-controlled trial. *Lancet Oncol* 2009; **10**: 25-34 [PMID: 19095497 DOI: 10.1016/S1470-2045(08)70285-7]

12 **Morgan B**, Thomas AL, Drevs J, Hennig J, Buchert M, Jivan A, Horsfield MA, Mross K, Ball HA, Lee L, Mietlowski W, Fuxuis S, Unger C, O'Byrne K, Henry A, Cherryman GR, Laurent D, Dugan M, Marmé D, Steward WP. Dynamic contrast-enhanced magnetic resonance imaging as a biomarker for the pharmacological response of PTK787/ZK 222584, an inhibitor of the vascular endothelial growth factor receptor tyrosine kinases, in patients with advanced colorectal cancer and liver metastases: results from two phase I studies. *J Clin Oncol* 2003; **21**: 3955-3964 [PMID: 14517187 DOI: 10.1200/JCO.2003.08.092]

13 **Herbst RS**, Hong D, Chap L, Kurzrock R, Jackson E, Silverman JM, Rasmussen E, Sun YN, Zhong D, Hwang YC, Evelhoch JL, Oliner JD, Le N, Rosen LS. Safety, pharmacokinetics, and antitumor activity of AMG 386, a selective angiopoietin inhibitor, in adult patients with advanced solid tumors. *J Clin Oncol* 2009; **27**: 3557-3565 [PMID: 19546406 DOI: 10.1200/JCO.2008.19.6683]

14 **Drevs J**, Siegert P, Medinger M, Mross K, Strecker R, Zirrgiebel U, Harder J, Blum H, Robertson J, Jürgensmeier JM, Puchalski TA, Young H, Saunders O, Unger C. Phase I clinical study of AZD2171, an oral vascular endothelial growth factor signaling inhibitor, in patients with advanced solid tumors. *J Clin Oncol* 2007; **25**: 3045-3054 [PMID: 17634482 DOI: 10.1200/JCO.2006.07.2066]

15 **Türkbey B**, Thomasson D, Pang Y, Bernardo M, Choyke PL. The role of dynamic contrast-enhanced MRI in cancer diagnosis and treatment. *Diagn Interv Radiol* 2010; **16**: 186-192 [PMID: 19885783 DOI: 10.4261/1305-3825.DIR.2537-08.1]

16 **O'Connor JP**, Jackson A, Parker GJ, Jayson GC. DCE-MRI biomarkers in the clinical evaluation of antiangiogenic and vascular disrupting agents. *Br J Cancer* 2007; **96**: 189-195 [PMID: 17211479 DOI: 10.1038/sj.bjc.6603515]

17 **Leach MO**, Morgan B, Tofts PS, Buckley DL, Huang W, Horsfield MA, Chenevert TL, Collins DJ, Jackson A, Lomas D, Whitcher B, Clarke L, Plummer R, Judson I, Jones R, Alonzi

R, Brunner T, Koh DM, Murphy P, Waterton JC, Parker G, Graves MJ, Scheenen TW, Redpath TW, Orton M, Karczmar G, Huisman H, Barentsz J, Padhani A. Imaging vascular function for early stage clinical trials using dynamic contrast-enhanced magnetic resonance imaging. *Eur Radiol* 2012; **22**: 1451-1464 [PMID: 22562143 DOI: 10.1007/s00330-012-2446-x]

18 **Wedam SB**, Low JA, Yang SX, Chow CK, Choyke P, Danforth D, Hewitt SM, Berman A, Steinberg SM, Liewehr DJ, Plehn J, Doshi A, Thomasson D, McCarthy N, Koeppen H, Sherman M, Zujewski J, Camphausen K, Chen H, Swain SM. Antiangiogenic and antitumor effects of bevacizumab in patients with inflammatory and locally advanced breast cancer. *J Clin Oncol* 2006; **24**: 769-777 [PMID: 16391297 DOI: 10.1200/JCO.2005.03.4645]

19 **Pickles MD**, Manton DJ, Lowry M, Turnbull LW. Prognostic value of pre-treatment DCE-MRI parameters in predicting disease free and overall survival for breast cancer patients undergoing neoadjuvant chemotherapy. *Eur J Radiol* 2009; **71**: 498-505 [PMID: 18572340 DOI: 10.1016/j.ejrad.2008.05.007]

20 **Flaherty KT**, Rosen MA, Heitjan DF, Gallagher ML, Schwartz B, Schnall MD, O'Dwyer PJ. Pilot study of DCE-MRI to predict progression-free survival with sorafenib therapy in renal cell carcinoma. *Cancer Biol Ther* 2008; **7**: 496-501 [PMID: 18219225]

21 **Jarnagin WR**, Schwartz LH, Gultekin DH, Gönen M, Haviland D, Shia J, D'Angelica M, Fong Y, Dematteo R, Tse A, Blumgart LH, Kemeny N. Regional chemotherapy for unresectable primary liver cancer: results of a phase II clinical trial and assessment of DCE-MRI as a biomarker of survival. *Ann Oncol* 2009; **20**: 1589-1595 [PMID: 19491285 DOI: 10.1093/annonc/mdp029]

22 **Taouli B**, Johnson RS, Hajdu CH, Oei MT, Merad M, Yee H, Rusinek H. Hepatocellular carcinoma: perfusion quantification with dynamic contrast-enhanced MRI. *AJR Am J Roentgenol* 2013; **201**: 795-800 [PMID: 24059368 DOI: 10.2214/AJR.12.9798]

23 **Liang PC**, Ch'ang HJ, Hsu C, Tseng SS, Shih TT, Wu Liu T. Dynamic MRI signals in the second week of radiotherapy relate to treatment outcomes of hepatocellular carcinoma: a preliminary result. *Liver Int* 2007; **27**: 516-528 [PMID: 17403192 DOI: 10.1111/j.1478-3231.2007.01456.x]

24 **Ingrisch M**, Sourbron S. Tracer-kinetic modeling of dynamic contrast-enhanced MRI and CT: a primer. *J Pharmacokinet Pharmacodyn* 2013; **40**: 281-300 [PMID: 23563847 DOI: 10.1007/s10928-013-9315-3]

25 **Brix G**, Griebel J, Kiessling F, Wenz F. Tracer kinetic modelling of tumour angiogenesis based on dynamic contrast-enhanced CT and MRI measurements. *Eur J Nucl Med Mol Imaging* 2010; **37** Suppl 1: S30-S51 [PMID: 20503049 DOI: 10.1007/s00259-010-1448-7]

26 **Verma S**, Turkbey B, Muradyan N, Rajesh A, Cornud F, Haider MA, Choyke PL, Harisinghani M. Overview of dynamic contrast-enhanced MRI in prostate cancer diagnosis and management. *AJR Am J Roentgenol* 2012; **198**: 1277-1288 [PMID: 22623539 DOI: 10.2214/AJR.12.8510]

27 **Sourbron S**. Technical aspects of MR perfusion. *Eur J Radiol* 2010; **76**: 304-313 [PMID: 20363574 DOI: 10.1016/j.ejrad.2010.02.017]

28 **Barrett T**, Brechbiel M, Bernardo M, Choyke PL. MRI of tumor angiogenesis. *J Magn Reson Imaging* 2007; **26**: 235-249 [PMID: 17623889 DOI: 10.1002/jmri.20991]

29 **Essig M**, Shiroishi MS, Nguyen TB, Saake M, Provenzale JM, Enterline D, Anzalone N, Dörfler A, Rovira A, Wintermark M, Law M. Perfusion MRI: the five most frequently asked technical questions. *AJR Am J Roentgenol* 2013; **200**: 24-34 [PMID: 23255738 DOI: 10.2214/AJR.12.9543]

30 **Sourbron SP**, Buckley DL. Tracer kinetic modelling in MRI: estimating perfusion and capillary permeability. *Phys Med Biol* 2012; **57**: R1-33 [PMID: 22173205 DOI: 10.1088/0031-9155/57/2/R1]

31 **Koh TS**, Bisdas S, Koh DM, Thng CH. Fundamentals of trac-

er kinetics for dynamic contrast-enhanced MRI. *J Magn Reson Imaging* 2011; **34**: 1262-1276 [PMID: 21972053 DOI: 10.1002/jmri.22795]

32 **Peng SL**, Chen CF, Liu HL, Lui CC, Huang YJ, Lee TH, Chang CC, Wang FN. Analysis of parametric histogram from dynamic contrast-enhanced MRI: application in evaluating brain tumor response to radiotherapy. *NMR Biomed* 2012; Epub ahead of print [PMID: 23073840 DOI: 10.1002/nbm.2882]

33 **Alic L**, van Vliet M, van Dijke CF, Eggermont AM, Veenland JF, Niessen WJ. Heterogeneity in DCE-MRI parametric maps: a biomarker for treatment response? *Phys Med Biol* 2011; **56**: 1601-1616 [PMID: 21335648 DOI: 10.1088/0031-9155/56/6/006]

34 **Rose CJ**, Mills SJ, O'Connor JP, Buonaccorsi GA, Roberts C, Watson Y, Cheung S, Zhao S, Whitcher B, Jackson A, Parker GJ. Quantifying spatial heterogeneity in dynamic contrast-enhanced MRI parameter maps. *Magn Reson Med* 2009; **62**: 488-499 [PMID: 19466747 DOI: 10.1002/mrm.22003]

35 **Rose CJ**, Mills S, O'Connor JP, Buonaccorsi GA, Roberts C, Watson Y, Whitcher B, Jayson G, Jackson A, Parker GJ. Quantifying heterogeneity in dynamic contrast-enhanced MRI parameter maps. *Med Image Comput Comput Assist Interv* 2007; **10**: 376-384 [PMID: 18044591]

36 **Ingrisch M**, Dietrich O, Attenberger UI, Nikolaou K, Sourbron S, Reiser MF, Fink C. Quantitative pulmonary perfusion magnetic resonance imaging: influence of temporal resolution and signal-to-noise ratio. *Invest Radiol* 2010; **45**: 7-14 [PMID: 19996761 DOI: 10.1097/RLI.0b013e3181bc2d0c]

37 **Roberts C**, Buckley DL, Parker GJ. Comparison of errors associated with single- and multi-bolus injection protocols in low-temporal-resolution dynamic contrast-enhanced tracer kinetic analysis. *Magn Reson Med* 2006; **56**: 611-619 [PMID: 16858671 DOI: 10.1002/mrm.20971]

38 **Luypaert R**, Sourbron S, de Mey J. Validity of perfusion parameters obtained using the modified Tofts model: a simulation study. *Magn Reson Med* 2011; **65**: 1491-1497 [PMID: 21500273 DOI: 10.1002/mrm.22728]

39 **Melbourne A**, Hipwell J, Modat M, Mertzanidou T, Huisman H, Ourselin S, Hawkes DJ. The effect of motion correction on pharmacokinetic parameter estimation in dynamic-contrast-enhanced MRI. *Phys Med Biol* 2011; **56**: 7693-7708 [PMID: 22086390 DOI: 10.1088/0031-9155/56/24/001]

40 **Kety SS**. The theory and applications of the exchange of inert gas at the lungs and tissues. *Pharmacol Rev* 1951; **3**: 1-41 [PMID: 14833874]

41 **Tofts PS**, Wicks DA, Barker GJ. The MRI measurement of NMR and physiological parameters in tissue to study disease process. *Prog Clin Biol Res* 1991; **363**: 313-325 [PMID: 1988983]

42 **Brix G**, Semmler W, Port R, Schad LR, Layer G, Lorenz WJ. Pharmacokinetic parameters in CNS Gd-DTPA enhanced MR imaging. *J Comput Assist Tomogr* 1991; **15**: 621-628 [PMID: 2061479]

43 **Larsson HB**, Stubgaard M, Frederiksen JL, Jensen M, Henriksen O, Paulson OB. Quantitation of blood-brain barrier defect by magnetic resonance imaging and gadolinium-DTPA in patients with multiple sclerosis and brain tumors. *Magn Reson Med* 1990; **16**: 117-1131 [PMID: 2255233 DOI: 10.1002/mrm.1910160111]

44 **Materne R**, Smith AM, Peeters F, Dehoux JP, Keyeux A, Horsmans Y, Van Beers BE. Assessment of hepatic perfusion parameters with dynamic MRI. *Magn Reson Med* 2002; **47**: 135-142 [PMID: 11754452]

45 **Chen BB**, Hsu CY, Yu CW, Wei SY, Kao JH, Lee HS, Shih TT. Dynamic contrast-enhanced magnetic resonance imaging with Gd-EOB-DTPA for the evaluation of liver fibrosis in chronic hepatitis patients. *Eur Radiol* 2012; **22**: 171-180 [PMID: 21879400 DOI: 10.1007/s00330-011-2249-5]

46 **Annet L**, Materne R, Danse E, Jamart J, Horsmans Y, Van Beers BE. Hepatic flow parameters measured with MR imag-

ing and Doppler US: correlations with degree of cirrhosis and portal hypertension. *Radiology* 2003; **229**: 409-414 [PMID: 12970464 DOI: 10.1148/radiol.2292021128]

47   **Baxter S**, Wang ZJ, Joe BN, Qayyum A, Taouli B, Yeh BM. Timing bolus dynamic contrast-enhanced (DCE) MRI assessment of hepatic perfusion: Initial experience. *J Magn Reson Imaging* 2009; **29**: 1317-1322 [PMID: 19472388 DOI: 10.1002/jmri.21795]

48   **Hagiwara M**, Rusinek H, Lee VS, Losada M, Bannan MA, Krinsky GA, Taouli B. Advanced liver fibrosis: diagnosis with 3D whole-liver perfusion MR imaging--initial experience. *Radiology* 2008; **246**: 926-934 [PMID: 18195377 DOI: 10.1148/radiol.2463070077]

49   **Nilsson H**, Nordell A, Vargas R, Douglas L, Jonas E, Blomqvist L. Assessment of hepatic extraction fraction and input relative blood flow using dynamic hepatocyte-specific contrast-enhanced MRI. *J Magn Reson Imaging* 2009; **29**: 1323-1331 [PMID: 19472389 DOI: 10.1002/jmri.21801]

50   **Choi SH**, Chung JW, Kim HC, Baek JH, Park CM, Jun S, Kim MU, Lee ES, Cho HR, Jae HJ, Lee W, Park JH. The role of perfusion CT as a follow-up modality after transcatheter arterial chemoembolization: an experimental study in a rabbit model. *Invest Radiol* 2010; **45**: 427-436 [PMID: 20440211 DOI: 10.1097/RLI.0b013e3181e07516]

51   **Martí-Bonmatí L**, Sanz-Requena R, Alberich-Bayarri A. Pharmacokinetic MR analysis of the cartilage is influenced by field strength. *Eur J Radiol* 2008; **67**: 448-452 [PMID: 18434058 DOI: 10.1016/j.ejrad.2008.02.047]

52   **Jaspers K**, Aerts HJ, Leiner T, Oostendorp M, van Riel NA, Post MJ, Backes WH. Reliability of pharmacokinetic parameters: small vs. medium-sized contrast agents. *Magn Reson Med* 2009; **62**: 779-787 [PMID: 19623622 DOI: 10.1002/mrm.22035]

53   **Abdullah SS**, Pialat JB, Wiart M, Duboeuf F, Mabrut JY, Bancel B, Rode A, Ducerf C, Baulieux J, Berthezene Y. Characterization of hepatocellular carcinoma and colorectal liver metastasis by means of perfusion MRI. *J Magn Reson Imaging* 2008; **28**: 390-395 [PMID: 18666145 DOI: 10.1002/jmri.21429]

54   **Miyazaki K**, Orton MR, Davidson RL, d'Arcy JA, Lewington V, Koh TS, Thng CH, Leach MO, Collins DJ, Koh DM. Neuroendocrine tumor liver metastases: use of dynamic contrast-enhanced MR imaging to monitor and predict radiolabeled octreotide therapy response. *Radiology* 2012; **263**: 139-148 [PMID: 22344403 DOI: 10.1148/radiol.12110770]

55   **Wang J**, Chen LT, Tsang YM, Liu TW, Shih TT. Dynamic contrast-enhanced MRI analysis of perfusion changes in advanced hepatocellular carcinoma treated with an antiangiogenic agent: a preliminary study. *AJR Am J Roentgenol* 2004; **183**: 713-719 [PMID: 15333360 DOI: 10.2214/ajr.183.3.1830713]

56   **Zhu AX**, Sahani DV, Duda DG, di Tomaso E, Ancukiewicz M, Catalano OA, Sindhwani V, Blaszkowsky LS, Yoon SS, Lahdenranta J, Bhargava P, Meyerhardt J, Clark JW, Kwak EL, Hezel AF, Miksad R, Abrams TA, Enzinger PC, Fuchs CS, Ryan DP, Jain RK. Efficacy, safety, and potential biomarkers of sunitinib monotherapy in advanced hepatocellular carcinoma: a phase II study. *J Clin Oncol* 2009; **27**: 3027-3035 [PMID: 19470923 DOI: 10.1200/JCO.2008.20.9908]

57   **Yopp AC**, Schwartz LH, Kemeny N, Gultekin DH, Gönen M, Bamboat Z, Shia J, Haviland D, D'Angelica MI, Fong Y, DeMatteo RP, Allen PJ, Jarnagin WR. Antiangiogenic therapy for primary liver cancer: correlation of changes in dynamic contrast-enhanced magnetic resonance imaging with tissue hypoxia markers and clinical response. *Ann Surg Oncol* 2011; **18**: 2192-2199 [PMID: 21286939 DOI: 10.1245/s10434-011-1570-1]

58   **Hsu CY**, Shen YC, Yu CW, Hsu C, Hu FC, Hsu CH, Chen BB, Wei SY, Cheng AL, Shih TT. Dynamic contrast-enhanced magnetic resonance imaging biomarkers predict survival and response in hepatocellular carcinoma patients treated with sorafenib and metronomic tegafur/uracil. *J Hepatol* 2011; **55**: 858-865 [PMID: 21338641 DOI: 10.1016/j.jhep.2011.01.032]

59   **Hsu C**, Yang TS, Huo TI, Hsieh RK, Yu CW, Hwang WS, Hsieh TY, Huang WT, Chao Y, Meng R, Cheng AL. Vandetanib in patients with inoperable hepatocellular carcinoma: a phase II, randomized, double-blind, placebo-controlled study. *J Hepatol* 2012; **56**: 1097-1103 [PMID: 22245891 DOI: 10.1016/j.jhep.2011.12.013]

60   **Sahani DV**, Holalkere NS, Mueller PR, Zhu AX. Advanced hepatocellular carcinoma: CT perfusion of liver and tumor tissue--initial experience. *Radiology* 2007; **243**: 736-743 [PMID: 17517931 DOI: 10.1148/radiol.2433052020]

61   **Ippolito D**, Sironi S, Pozzi M, Antolini L, Ratti L, Meloni F, Invernizzi F, Valsecchi MG, Fazio F. Perfusion computed tomographic assessment of early hepatocellular carcinoma in cirrhotic liver disease: initial observations. *J Comput Assist Tomogr* 2008; **32**: 855-858 [PMID: 19204443 DOI: 10.1097/RCT.0b013e318161dc58]

62   **Ippolito D**, Sironi S, Pozzi M, Antolini L, Invernizzi F, Ratti L, Leone EB, Fazio F. Perfusion CT in cirrhotic patients with early stage hepatocellular carcinoma: assessment of tumor-related vascularization. *Eur J Radiol* 2010; **73**: 148-152 [PMID: 19054640 DOI: 10.1016/j.ejrad.2008.10.014]

63   **Chen YW**, Pan HB, Tseng HH, Hung YT, Huang JS, Chou CP. Assessment of blood flow in hepatocellular carcinoma: correlations of computed tomography perfusion imaging and circulating angiogenic factors. *Int J Mol Sci* 2013; **14**: 17536-17552 [PMID: 23985826 DOI: 10.3390/ijms140917536]

64   **Ippolito D**, Sironi S, Pozzi M, Antolini L, Ratti L, Alberzoni C, Leone EB, Meloni F, Valsecchi MG, Fazio F. Hepatocellular carcinoma in cirrhotic liver disease: functional computed tomography with perfusion imaging in the assessment of tumor vascularization. *Acad Radiol* 2008; **15**: 919-927 [PMID: 18572129 DOI: 10.1016/j.acra.2008.02.005]

65   **Ippolito D**, Capraro C, Casiraghi A, Cestari C, Sironi S. Quantitative assessment of tumour associated neovascularisation in patients with liver cirrhosis and hepatocellular carcinoma: role of dynamic-CT perfusion imaging. *Eur Radiol* 2012; **22**: 803-811 [PMID: 22086560 DOI: 10.1007/s00330-011-2307-z]

66   **Faivre S**, Zappa M, Vilgrain V, Boucher E, Douillard JY, Lim HY, Kim JS, Im SA, Kang YK, Bouattour M, Dokmak S, Dreyer C, Sablin MP, Serrate C, Cheng AL, Lanzalone S, Lin X, Lechuga MJ, Raymond E. Changes in tumor density in patients with advanced hepatocellular carcinoma treated with sunitinib. *Clin Cancer Res* 2011; **17**: 4504-4512 [PMID: 21531821 DOI: 10.1158/1078-0432.CCR-10-1708]

67   **Jiang T**, Kambadakone A, Kulkarni NM, Zhu AX, Sahani DV. Monitoring response to antiangiogenic treatment and predicting outcomes in advanced hepatocellular carcinoma using image biomarkers, CT perfusion, tumor density, and tumor size (RECIST). *Invest Radiol* 2012; **47**: 11-17 [PMID: 21512396 DOI: 10.1097/RLI.0b013e3182199bb5]

68   **Stewart EE**, Sun H, Chen X, Schafer PH, Chen Y, Garcia BM, Lee TY. Effect of an angiogenesis inhibitor on hepatic tumor perfusion and the implications for adjuvant cytotoxic therapy. *Radiology* 2012; **264**: 68-77 [PMID: 22627603 DOI: 10.1148/radiol.12110674]

69   **Messiou C**, Orton M, Ang JE, Collins DJ, Morgan VA, Mears D, Castellano I, Papadatos-Pastos D, Brunetto A, Tunariu N, Mann H, Tessier J, Young H, Ghiorghiu D, Marley S, Kaye SB, deBono JS, Leach MO, deSouza NM. Advanced solid tumors treated with cediranib: comparison of dynamic contrast-enhanced MR imaging and CT as markers of vascular activity. *Radiology* 2012; **265**: 426-436 [PMID: 22891356 DOI: 10.1148/radiol.12112565]

70   **Galbraith SM**, Lodge MA, Taylor NJ, Rustin GJ, Bentzen S, Stirling JJ, Padhani AR. Reproducibility of dynamic contrast-enhanced MRI in human muscle and tumours: comparison of quantitative and semi-quantitative analysis. *NMR Biomed* 2002; **15**: 132-142 [PMID: 11870909]

71   **Murphy P**, Koh DM. Imaging in clinical trials. *Cancer Imaging*

2010; **10** Spec no A: S74-S82 [PMID: 20880784 DOI: 10.1102/1 470-7330.2010.9027]

72 **Ng CS**, Raunig DL, Jackson EF, Ashton EA, Kelcz F, Kim KB, Kurzrock R, McShane TM. Reproducibility of perfusion parameters in dynamic contrast-enhanced MRI of lung and liver tumors: effect on estimates of patient sample size in clinical trials and on individual patient responses. *AJR Am J Roentgenol* 2010; **194**: W134-W140 [PMID: 20093564 DOI: 10.2214/AJR.09.3116]

73 **Leach MO**, Brindle KM, Evelhoch JL, Griffiths JR, Horsman MR, Jackson A, Jayson GC, Judson IR, Knopp MV, Maxwell RJ, McIntyre D, Padhani AR, Price P, Rathbone R, Rustin GJ, Tofts PS, Tozer GM, Vennart W, Waterton JC, Williams SR, Workman P. The assessment of antiangiogenic and antivascular therapies in early-stage clinical trials using magnetic resonance imaging: issues and recommendations. *Br J Cancer* 2005; **92**: 1599-1610 [PMID: 15870830 DOI: 10.1038/sj.bjc.6602550]

百世登

Baishideng®

ISSN 1007-9327

12>

9 771007 932045